Available online at www.sciencedirect.com

ScienceDirect

Proceedings of the Combustion Institute 39 (2023) 673–684

Proceedings of the Combustion Institute

www.elsevier.com/locate/proci

Understanding the low-temperature chemistry of 1,2,4-trimethylbenzene

Shijun Dong [a], Goutham Kukkadapu [b], Jinhu Liang [c,*], Xiaobei Cheng [a], Scott W. Wagnon [b,*], William J. Pitz [b], Henry J. Curran [d]

[a] *State Key Laboratory of Coal Combustion, School of Energy and Power Engineering, Huazhong University of Science and Technology, Wuhan, Hubei, China*

[b] *Materials Science Division, Lawrence Livermore National Laboratory, Livermore, USA*

[c] *School of Environmental and Safety Engineering, North University of China, Taiyuan, 030051, China*

[d] *Combustion Chemistry Centre, School of Biological and Chemical Sciences, Ryan Institute, MaREI, University of Galway, Galway, Ireland*

Received 5 January 2022; accepted 17 August 2022
Available online 9 December 2022

Abstract

1,2,4-trimethylbenzene is an important representative aromatic component of gasoline/diesel/jet fuels and thus it is necessary to understand its low-temperature chemistry. In this paper, ignition delay times (IDTs) of both 1,2,4-trimethylbenzene (124TMB) and its blends with *n*-heptane were measured at engine-like conditions using both a high-pressure shock tube and a rapid compression machine for fuel in 'air' mixtures at pressures of 10 and 30 atm and at temperatures in the range 600 – 1100 K. The experiments in this study show for the first time that 124TMB presents a two-stage ignition behavior at engine relevant conditions. Blending *n*-heptane with 124TMB can significantly increase mixture reactivity at temperatures below 1000 K. A new detailed mechanism has been developed to simulate the experimentally measured IDT data. The mechanism can capture well the two-stage ignition behavior as well as the ignition delays at different pressures, equivalence ratios over a wide temperature range, for both pure fuels and their blended mixtures. Flux analyses show that the benzylic radicals (formed via H-atom abstraction from the methyl groups ortho-sites on 124TMB) can add to O_2 forming $R\dot{O}_2$ radicals, which can isomerize to $\dot{Q}OOH$ by intramolecular H-atom transfer from the ortho- methyl group and these $\dot{Q}OOH$ radicals undergo a second addition to O_2. This is analogous to the chain branching reaction pathways of alkanes. The chain branching reaction pathways are responsible for the first-stage heat release of 124TMB. The competitions between chain branching and both chain propagating and chain termination reaction pathways lead to a less pronounced negative temperature coefficient (NTC) behavior for 124TMB oxidation, compared to two-stage ignition behavior observed for alkanes and other fuels.
Published by Elsevier Inc. on behalf of The Combustion Institute.

Keywords: 1,2,4-trimethylbenzene; Ignition delay times; Two-stage ignition; Kinetic modeling

https://doi.org/10.1016/j.proci.2022.08.106
1540-7489 Published by Elsevier Inc. on behalf of The Combustion Institute.

1. Introduction

Alkylated aromatic species comprise a significant portion of practical fuels [1,2], and the aromatic components are known major contributors to polycyclic aromatic hydrocarbon (PAH) formation [3]. The low-temperature chemistry of these alkylated aromatics is more complicated than for toluene and benzene [4], while their low-temperature chemistry is important as it directly affects fuel auto-ignition at engine relevant conditions. Therefore, toluene or benzene are not ideal representative aromatic components of practical fuels [2,5-8]. Hence, accurate kinetic models of alkylated aromatics are necessary to develop surrogate models which can be used to predict the combustion of real fuels in practical combustors.

Some alkylated aromatics, including xylenes [9–12], ethylbenzene [13], *n*-propylbenzene [14,15], 1,3,5-trimethylbenzene (135TMB) [5] and 124TMB [4,10,16], have been studied as surrogates for real fuels. Roubaud et al. [4] studied the auto-ignition behavior of 11 alkylbenzenes in a rapid compression machine (RCM) in the low-temperature region (600 – 900 K) at $p = 16$ bar. The experimental results show that toluene, *m*-xylene, *p*-xylene, and 135TMB ignite only at temperatures above 900 K. However, *o*-xylene, 1,2,3-trimethylbenzene (123TMB), 124TMB, *n*-propyl benzene, 2-ethyl toluene, and *n*–butyl benzene ignite at much lower temperatures and pressures. In the Roubaud et al. study, very limited IDTs for 124TMB were obtained at 800 – 900 K as the experimental pressure was too low (~16 bar). Meanwhile, the volume history profiles accounting for the facility effects during simulations were not provided. Kukkadapu et al. [10] recently studied the oxidation of toluene, o-xylene, and 124TMB using a rapid compression machine. These experiments were studied over a temperature range of 850 – 1050 K, at pressures of 25 – 45 atm, and $[O_2] \sim 12.5\%$. A kinetic model was also proposed by Kukkadapu et al. to simulate the oxidation of the methylated aromatics. However, due to dilution and temperatures higher than 850 K, the low-temperature chemistry of 124TMB could only be partially studied. Diévart et al. [5] proposed a new kinetic model of 135TMB based on new experimental data, including shock tube IDTs, laminar burning velocities and species profiles of fuel oxidation in a high-pressure flow reactor. Malewicki et al. [6] studied the oxidation behavior of 135TMB as a Jet A surrogate, and a kinetic model was developed. Ranzi et al. [7] proposed a reduced mechanism for fossil and biomass-derived transportation fuels. However, the chemistry of three TMB isomers were lumped in the published mechanism. Weng et al. [8] studied the oxidation behavior of 124TMB in a jet-stirred reactor at an equivalence ratio of 2.0 and at atmospheric pressure, in the temperature range 700 – 1100 K, and a kinetic model was developed to simulate these data. Moreover, both the rate constants and thermochemistry data for the 124TMB sub-mechanism were provided as Supplementary material but the full mechanism was not included.

124TMB has been chosen as a representative aromatic component in surrogate models for gasoline, jet, kerosene and diesel fuels [7,16-21], and these surrogate models can successfully reproduce many combustion characteristics of practical fuels. While 124TMB has been widely used in surrogate fuel models, little information is available in the literature on the oxidation of 124TMB at engine relevant high pressures, low temperatures, and air-like dilution conditions. Furthermore, we are not aware of any studies of the blending response of 124TMB with primary reference fuels (*n*-heptane or isooctane) which is needed to improve kinetic model development.

To address the lack of information on 124TMB oxidation characteristics, IDTs of 124TMB and its blends with *n*-heptane, have been measured at engine-like conditions using both a high-pressure shock tube (HPST) and an RCM, for fuel in 'air' mixtures at pressures of 10 and 30 atm and at temperatures in the range 600 – 1100 K. Additionally, a new and improved kinetic model describing 124TMB has been developed to simulate these data.

2. Experimental description

In this study, both the HPST and the RCM at the University of Galway (UG) were used to perform the experiments. Detailed descriptions of both facilities have been reported previously [22,23], thus only a brief description is included here. The HPST was used to measure IDTs of less than 3 ms which are too short to be reliably measured in the RCM. The HPST has an internal diameter of 63.5 mm and a total length of 8.76 m, and is divided into three parts: a 5.73 m long driven section, a 3.0 m long driver section and a 3.0 cm long double-diaphragm section. The incident shock velocity is determined using six pressure transducers (PCB, 113B24) installed in the sidewall, and another pressure transducer (Kistler 603C) installed in the endwall is used to determine the IDT. The temperature and pressure of the gas behind the reflected shock wave is calculated using GasEq [24] based on the measured incident shock velocity and initial conditions of temperature, pressure and mixture composition. The UG RCM has a twin-opposed piston configuration, with a fast compression time of approximately 16 ms. To im-

* Corresponding author.
E-mail addresses: jhliang@nuc.edu.cn (J. Liang), wagnon1@llnl.gov (S.W. Wagnon).

Table 1
Experimental conditions of the HPST and RCM (Species in percent mole fraction. p & T are at end of compression.).

No.	124TMB	NC7H16	O_2	N_2 + Ar + CO_2	φ, blending ratio	p / atm	T / K	Facility
1	0.867	–	20.818	78.315	0.5, 100% 124TMB	10, 30	700 – 1100 K	RCM
2	0.664	0.221	20.815	78.300	0.5, 75% 124TMB			RCM
3	0.452	0.452	20.811	78.284	0.5, 50% 124TMB			RCM & HPST
4	0.231	0.694	20.806	78.269	0.5, 25% 124TMB			HPST
5	1.720	–	20.639	77.641	1.0, 100% 124TMB			RCM
6	1.317	0.439	20.631	77.613	1.0, 75% 124TMB			RCM
7	0.897	0.897	20.623	77.583	1.0, 50% 124TMB			RCM & HPST
8	0.458	1.374	20.615	77.552	1.0, 25% 124TMB			HPST

prove post-compression temperature homogeneity, creviced pistons are employed. The geometric compression ratio is fixed in the experiments, and the initial temperature is varied to achieve different compressed gas temperatures. These are calculated using GasEq based on the measured compressed pressure and initial conditions of pressure, temperature and mixture composition.

The experimental conditions of the HPST and RCM experiments are given in Table 1. The IDTs of both pure 124TMB and various blends with *n*-heptane were measured for fuel/'air' mixtures at both 10 and 30 atm, over a wide temperature range (600 – 1100 K). In the experiments, 'air' refers to the diluent (nitrogen or argon) and oxygen in a ratio of 79:21. Due to the low-vapor pressure of 124TMB, only $\varphi = 0.5$ and 1.0 conditions were studied. The system was heated to 120 °C to ensure full fuel vaporization. In addition to the experiments with 124TMB in 'air' mixtures, we have also studied the ignition characteristics of 124TMB/*n*-heptane blends in 'air' to ensure that the blending response of 124TMB is accurately predicted by the model. We chose *n*-heptane as 124TMB is less reactive and thus adding *n*-heptane would enhance the reactivity of the mixtures.

The definitions of IDTs measured in both the HPST and RCM are shown in Fig. 1. Two-stage ignition behavior was observed in the pure 124TMB RCM experiments, Fig. 1(b). The definitions of 1st and 2nd stage IDT are also shown in Fig. 1(a) and (b). A 20% uncertainty is assigned to the IDT measurements in both facilities, as discussed in our previous study [25].

High purity 124TMB and *n*-heptane fuels (> 98.0%) were provided by Sigma-Aldrich. High purity oxygen (> 99%), nitrogen (> 99%), carbon dioxide (> 99%) and argon (> 99%) were provided by BOC.

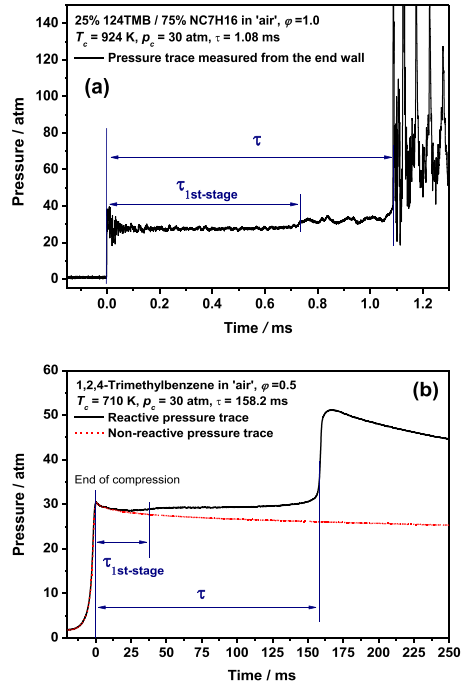

Fig. 1. Definition of ignition delay time measured in (a) a HPST and (b) an RCM.

3. Chemical kinetic model development

The kinetic model used here to simulate the oxidation of 124TMB/*n*-heptane mixtures is primarily based on *n*-heptane and LLNL aromatics mechanisms from the studies by Malliotakis et al. [26] and Kukkadapu et al. [10] respectively. These sub-mechanisms have been used earlier in the mod-

eling of the oxidation of multi-component gasoline surrogates [27]. While no changes were made to the *n*-heptane chemistry, the oxidation chemistry of aromatic radicals has been updated. Specifically, the chemistry related to the reactions of phenyl ($\dot{C}_6H_5$), methyl-phenyl ($CH_3\dot{C}_6H_4$) and dimethyl-phenyl radicals ($(CH_3)_2\dot{C}_6H_3$) with molecular oxygen were modified using recent kinetics from Morozov et al. [28]. These modifications were found to have a significant effect on the species profiles and flame structure predictions of laminar premixed benzene/propyne and toluene/propyne flames [29]. Furthermore, the reactions of $\dot{C}H_3$ radicals with methyl-phenyl ($CH_3\dot{C}_6H_4$) and dimethyl-phenyl ($(CH_3)_2\dot{C}_6H_3$) were updated in the present work to model the chemically activated pathways which were missing in the earlier mechanism of Kukkadapu et al. [10]. The oxidation of benzylic radicals by O_2 and $H\dot{O}_2$ was also modified in the present study. These modifications were primarily perturbations (within a factor of two) to the *A* factors of the important reaction pathways. Table 2 shows the rate constants and references of some important reactions. Chemkin-Pro [39] was used to perform all simulations presented here.

4. Results and discussion

4.1. Effects of pressure and equivalence ratio on the auto-ignition behavior of 124TMB

Fig. 2 shows the experimental and simulated results of pure 124TMB at different equivalence ratios and pressures in the low- to intermediate temperature region. The current model can capture well both the first-stage and total IDTs. The IDTs of pure 124TMB show significant sensitivities to experimental pressures, and the pressure effects are provided in Fig. S1. However, the fuel reactivity of pure 124TMB does not change significantly when the equivalence ratio increases from $\varphi = 0.5$ to 1.0, for both 15 and 30 atm. The current model can capture well both the equivalence ratio and pressure effects.

Fig. 3 shows pressure traces of pure 124TMB RCM experiments with two-stage ignition behavior, and the corresponding non-reactive pressure traces are also provided. Pressure traces showing two-stage ignition behavior for other conditions are provided as SM in Fig. S2. For the RCM experiments, at least two experiments were perfromed for each temperature point to ensure repeatability. Figs. 2 and 3 show that, despite the minor differences, the first-stage IDTs and the first-stage heat release are highly repeatable. Both the first-stage IDTs and first-stage heat release decrease with increasing temperatures, which is analogous the two-stage ignition behavior of alkanes.

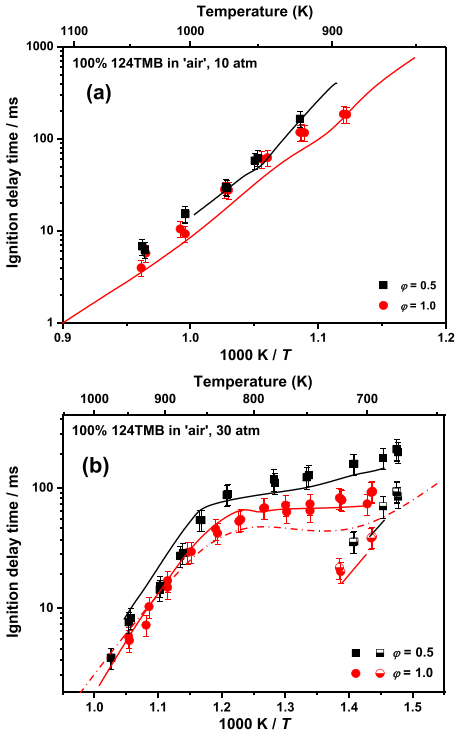

Fig. 2. Experimental and simulated results of pure 124TMB IDTs at different equivalence ratios. (a) 10 atm, (b) 30 atm. Solid symbols: RCM data. Half-filled symbols: first-stage IDT data. Solid lines: RCM simulations including facility effect. Dash dot line: constant volume simulations.

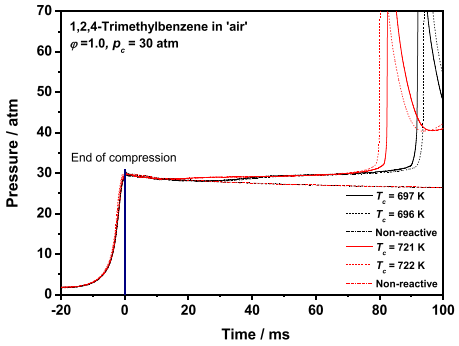

Fig. 3. Experimental pressure traces of pure 124TMB RCM experiments at different temperatures with two repeats.

The low-temperature heat release of in-cylinder gas is very important as it directly affects engine combustion phasing. Therefore, it is important that the low-temperature heat release should be validated for the major fuel components involved in a surrogate model. 124TMB is a representative component of alkylated aromatics, which comprise

Table 2
Rate constant parameters for the important reactions in the current model (units of cm^3, mol, s, cal).

No.	Reactions	A	n	E_a	Reference
1	T124MBZ+ȮH<=>*O*-XYLĊH_2+H_2O	3.54E+05	2.390	–602.	[30] [a]
2	T124MBZ+ȮH<=>*P*-XYLĊH_2+H_2O	1.77E+05	2.390	–602.	[30]
3	T124MBZ+O_2<=>*O*-XYLCH_2+HO_2	8.72E+07	2.500	46,000.	[31] [b]
4	T124MBZ+O_2<=> *P*-XYLĊH_2+HO_2	4.36E+07	2.500	46,000.	[31] [c]
5	*O*-XYLĊH_2+O_2<=>*O*-XYLCH_2OȮ	3.28E+46	–11.590	9000.	[32] [d]
	0.1 atm	2.82E+45	–10.974	9730.	
	1 atm	9.56E+38	–8.765	8430.	
	10 atm	4.60E+31	–6.360	6510.	
	100 atm				
6	*O*-XYLCH_2OȮ<=>*O*-ĊH_2TOLCH_2OOH	1.00E+09	0.850	20,800.	[33] [e]
7	*O*–ĊH_2TOLCH_2OOH<=>CH_3TOLETCOC+OH	2.28E+30	–5.400	29,800.	[32] [f]
8	*O*-ĊH_2TOLCH_2OOH+O_2=>O_2CH_2TOLCH_2OOH	3.28E+46	–11.590	9000.	[32] [d]
	0.1 atm	2.82E+45	–10.974	9730.	
	1 atm	9.56E+38	–8.765	8430.	
	10 atm	4.60E+31	–6.360	6510.	
	100 atm				
9	Ȯ$_2$CH_2TOLCH_2OOH=>*O*-ĊH_2TOLCH_2OOH+O_2	6.82E+45	–10.700	31,200.	[32] [g]
	0.1 atm	1.14E+46	–10.480	32,400.	
	1 atm	1.72E+46	–10.200	34,700.	
	10 atm	5.89E+46	–10.050	37,400.	
	100 atm				

(*continued on next page*)

Table 2 (*continued*)

No.	Reactions	*A*	*n*	E_a	Reference
10	$\dot{O}_2CH_2TOLCH_2OOH <=> \dot{O}H + TMBKET$	1.00E+09	0.850	19,800.	[33] [h]
11	*P*-$XYL\dot{C}H_2 + H\dot{O}_2 <=> P$-$XYLCH_2OOH$	3.75E+30	–6.000	2500.	Estimate [i]
12	*O*-$XYL\dot{C}H_2 + H\dot{O}_2 <=> O$-$XYLCH_2OOH$	3.75E+30	–6.000	2500.	Estimate [i]
13	$HOC_6H_4CH_3 + O_2 <=> OC_6H_4CH_3 + H\dot{O}_2$	1.00E+13	0.000	38,900.	[34]
14	*O*-$XYL\dot{C}H_2$+*P*-$XYL\dot{C}H_2 <=> TMBDIMER3$	1.15E+24	–3.784	2030.	[35] [j]
15	$NC_7H_{16} + \dot{O}H <=> \dot{C}_7H_{15}\text{–}2 + H_2O$	1.41E+10	0.935	505.	[36]
16	$NC_7H_{16} + \dot{O}H <=> \dot{C}_7H_{15}\text{–}1 + H_2O$	2.73E+07	1.813	868.	[36]
17	$H\dot{O}_2 + H\dot{O}_2 <=> H_2O_2 + O_2$	1.21E+10	0.422	–1481.	[37] [k]
	DUPLICATE	1.69E+16	–0.681	12,932.	
	DUPLICATE				

[a] The A-factor is multiplied by two to account for reaction path degeneracy.
[b] The A-factor is multiplied by two to account for reaction path degeneracy, and an additional factor of 2 as a local optimization.
[c] The A-factor is multiplied by two as a local optimization.
[d] The fitted rate constants are within a factor of 2 of the rate constants in Table 4 of Murakami et al. [32] for $C_6H_5\dot{C}H_2 + O_2 => C_6H_5CH_2O\dot{O}$. The high-pressure limit is used for the 100 atm PLOG entry.
[e] The A-factor is multiplied by two as a local optimization.
[f] The fitted rate constant parameters correspond to the high-pressure limit of channel G from Murakami et al. [32] with an A-factor divided by a factor of 4 as a local optimization.
[g] The fitted rate constants are within a factor of 1.5 of the rate constants in Table 4 of Murakami et al. [32] for $C_6H_5CH_2O\dot{O} => C_6H_5\dot{C}H_2 + O_2$. The high-pressure limit is used for the 100 atm PLOG entry.
[h] The A-factor is multiplied by two and the activation energy is lowered by 1 kcal/mol as local optimizations.
[i] The high temperature portion of this rate constant was reduced to account for the chemically activated pathway analogous to $C_6H_5\dot{C}H_2 + H\dot{O}_2 = C_6H_5CH_2\dot{O} + \dot{O}H$. The low temperature portion of the rate constant is in good agreement with the calculations of Da Silva and Bozzelli [38].
[j] The A-factor is 25% lower as a local optimization.
[k] As implemented in NUIGMech1.1.

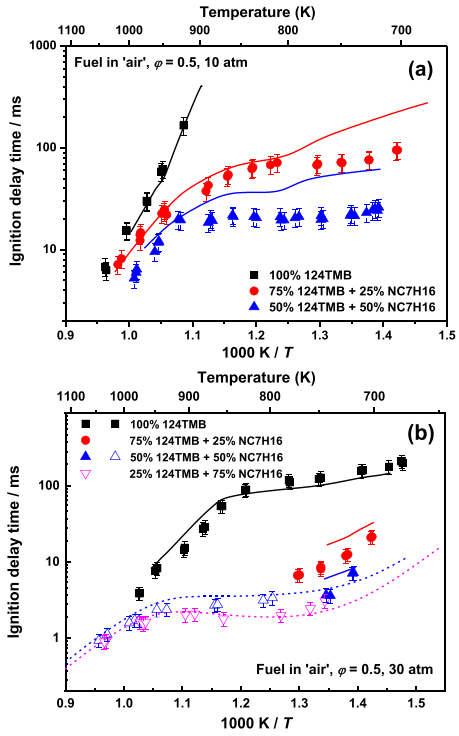

Fig. 4. Experimental and simulated results of 124TMB / *n*-heptane IDTs at φ=0.5. (a) 10 atm, (b) 30 atm. Solid symbols: RCM data. Open symbols: HPST data. Solid lines: RCM simulations including facility effect. Dashed lines: constant-volume simulations.

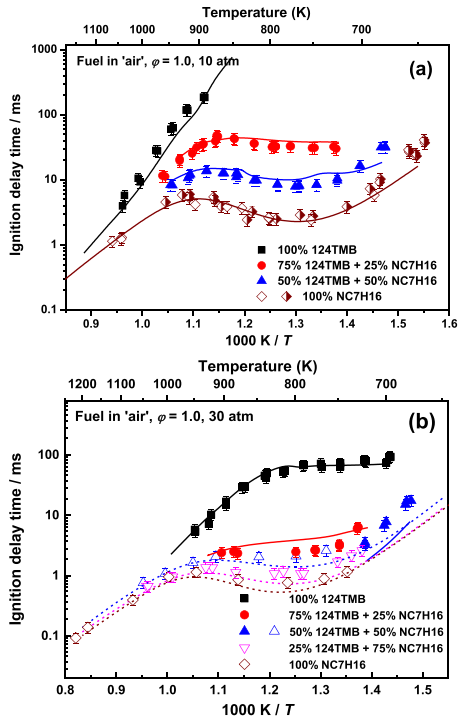

Fig. 5. Experimental and simulated results of 124TMB / *n*-heptane IDTs at φ=1. Solid symbols: RCM data. Open symbols: HPST data. Solid lines: RCM simulations including facility effect. Dashed lines: constant-volume simulations. 100% *n*-heptane from Silke et al. [40] and Heufer et al. [41].

over 30% (by weight on average) of diesel. Therefore, the low-temperature chemistry of 124TMB needs to be well validated. The low-temperature chemistry controlling the low-temperature heat release will be discussed in Section 4.3.

4.2. *Effects of blending n-heptane on the auto-ignition behavior of 124TMB*

Figs. 4 and 5 show the experimental and simulated results for the pure fuels and their mixtures at different blending ratios, equivalence ratios and pressures, in the low- to intermediate-temperature range of 650 – 1200 K. Blending *n*-heptane with 124TMB significantly increases mixture reactivity at temperatures below 1000 K, and at higher temperatures *n*-heptane slightly increases the reactivity. 650–1200 K is the gas temperature range of engines when auto-ignition occurs. Therefore, it is important for kinetic models to capture the auto-ignition behavior of fuel reactivity in this temperature range.

In Figs. 4 and 5, the fuel reactivity of 124TMB / *n*-heptane blends increases significantly as the *n*-heptane mole fraction increases from zero to 25%, with the measured IDTs decreasing by more than an order of magnitude compared to pure 124TMB. As the mole fraction of *n*-heptane increases from 25% to 50% the measured IDTs decrease further by a factor of two to three. The 124TMB/*n*-heptane blends show a more pronounced NTC behavior as the mole fraction of *n*-heptane increases in the mixture. For the φ = 0.5, 10 atm mixture, the model predictions are slow by a factor of two at temperatures below 800 K. For the φ = 1.0, 30 atm mixture, the model predictions are slightly faster compared to the experiments in the NTC region, as both the 124TMB and *n*-heptane models are slightly faster in this temperature range. The validation results of the current model compared to literature data are also provided as Supplementary material. Overall, the current model can capture well the auto-ignition behavior of different 124TMB/*n*-heptane blends at the conditions studied.

4.3. *Flux and sensitivity analyses*

Fig. 6 shows the flux analyses results for the oxidation of both pure 124TMB and 124TMB/*n*-heptane blends at 700 and 800 K. These temperatures were chosen as they correspond to temper-

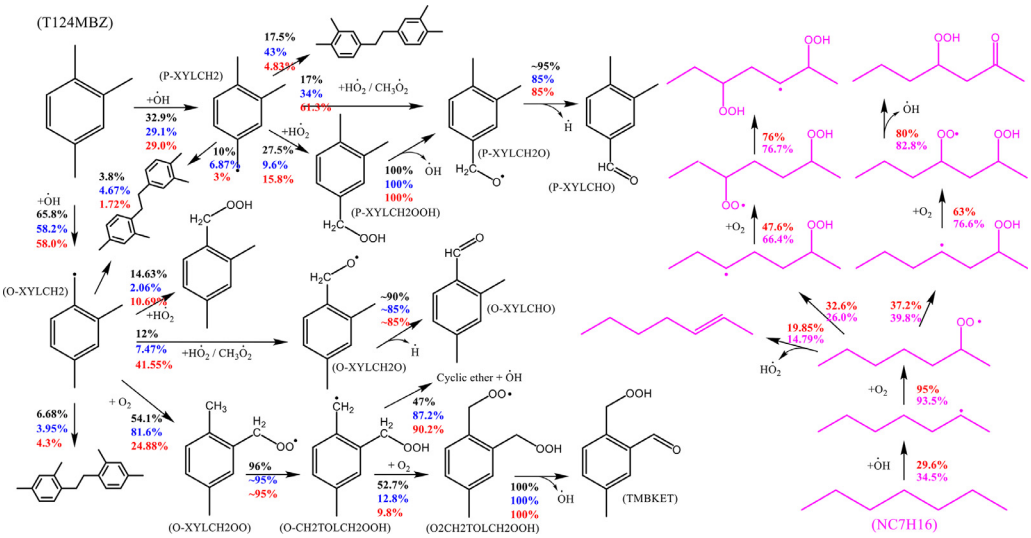

Fig. 6. Flux analyses based on constant volume simulations for 124TMB, *n*-heptane and 75%/25% 124TMB/*n*-heptane blends at $\varphi = 1.0$ in 'air', $p = 30$ atm and 20% 124TMB/*n*-heptane consumption. The benzylic radicals produced by H-atom abstraction from the methyl groups at the 1 and 2 position (ortho-sites) are lumped. Numbers represent the percentage of flux that goes into a particular species. Black and blue numbers represent fuel flux at 700 K and 800 K for pure 124TMB. Red numbers represent fuel flux at 800 K for 75%/25% 124TMB/*n*-heptane blends. Magenta numbers represent fuel flux at 800 K for pure *n*-heptane blends.

atures with two-stage and NTC ignition behavior, Fig. 2(b).

For pure 124TMB oxidation, over 97% of the fuel is consumed via H-atom abstraction from the methyl sites by ȮH radicals. In the current model, reactions of both H-atom abstraction by ȮH radicals and ȮH addition to the ring have been included according to the study of Seta et al. [30]. However, the flux analysis results show that the ȮH addition reactions are not important at the conditions studied. H-atom abstractions by ȮH radicals lead to the formation of two benzylic radicals, O-XYLĊH_2 and P-XYLĊH_2. The radicals produced by H-atom abstraction from the methyl groups at the 1 and 2 position (ortho-sites) are lumped to decrease the mechanism size and hence only one radical (O-XYĊH_2) is shown in Fig. 6. At the time corresponding to 20% fuel consumption, the flux results show that both benzylic radicals exhibit some similarities; they react with HȮ$_2$ radicals and undergo radical recombination. The reactions with HȮ$_2$ radicals mainly produce ȮH radicals, which is chain propagating. However, the reactions of radical recombination are chain terminating as they produce stable tetramethyl-bibenzyl species.

The O-XYĊH_2 radicals can also add to O_2 forming RȮ$_2$ (O-XYCH_2OȮ), which can isomerize to ȮQOOH (O–CH_2TOLCH_2OOH) by H-transfer from the nearby methyl group. These ȮQOOH radicals can either undergo chain propagation reactions to produce cyclic ethers and ȮH radicals, or they can undergo a second addition with O_2, with the Ȯ$_2$QOOH radicals so formed generating ketohydroperoxide (KHP or specifically TMBKET), which is chain branching, Fig. 6. TMBKET subsequently decomposes to produce 4-methylphthalaldehyde along with ȮH radicals and Ḣ atoms. The decomposition of TMBKET is the main source of both ȮH and Ḣ at low temperatures. Thus, the peroxy chemistry initiated from formation of O-XYĊH_2 leads to chain branching reaction pathways resulting in ignition at relatively lower temperatures, and this is consistent with the experimental results of Roubaud et al. [4]. The experimental results show that alkylbenzenes with ortho- alkyl/methyl groups, including *o*-xylene, 1,2,3-trimethylbenzene, 1,2,4-trimethylbenzene, 2-ethyltoluene, can ignite at lower temperatures. However, alkylbenzenes without ortho- alkyl/methyl groups, including toluene, *m*-xylene, *p*-xylene, and 1,3,5-trimethylbenzene, only ignite at higher temperatures.

For pure 124TMB oxidation, as the temperature increases from 700 to 800 K, the flux through O_2 addition to O-XYLĊH_2 radical increases, while the flux through reactions with HȮ$_2$ decreases. This is because as the temperature increases the RȮ$_2$ (O-XYCH_2OȮ) pathways and subsequent chain-branching pathways (e.g. TMBKET formation and decomposition) decrease. At higher temperatures

(800 K at 30 atm) the flux to cyclic ether formation also increases. The reduced production of TMBKET results in less production of $\dot{H}$ atoms which are a primary driver in the formation of $H\dot{O}_2$ radicals. Thus, the flux through $XYL\dot{C}H_2$ radicals with $H\dot{O}_2$ decreases, and the flux through reactions with O_2 increases with temperature. Additionally, the increased formation of cyclic ether (chain propagating) and reduced formation of TMBKET (chain branching) leads to an NTC like response in 124TMB oxidation as shown in Fig. 2(b).

Fig. 6 also shows the flux for the 124TMB/*n*-heptane blends. As the low-temperature reaction pathways of *n*-heptane are well known, only a reduced flux analysis showing one of the major channels is given. As can be seen, a large portion of heptyl radicals undergo chain branching reaction pathways, which produce $\dot{O}H$ radicals and hence increase reactivity. Meanwhile, the presence of *n*-heptane also promotes $H\dot{O}_2$ formation via $H\dot{O}_2$ elimination from $R\dot{O}_2$. Therefore, the flux of benzylic radicals reacting with $H\dot{O}_2$ increases and the overall flux of benzylic radical recombination decreases.

To explain the two-stage ignition behavior of 124TMB at low temperatures, it is important to analyze the reactions contributing to the first-stage heat release. The reaction of $\dot{H} + O_2 (+M) \langle = \rangle H\dot{O}_2 (+M)$ contributes up to 28%. The chain branching reaction pathways, starting from $O\text{-}XY\dot{C}H_2$ formation to the decomposition of TMBKET, contribute approximately 18% of first-stage heat release. Meanwhile, the decomposition of the TMBKET accounts for over 50% of $\dot{H}$ atom formation. The reactions of two benzylic radicals with $H\dot{O}_2$ also contributes approximately 12% to the first-stage heat release. Moreover, the chain branching reaction pathways of $\dot{O}_2QOOH$ isomerization and KHP decomposition efficiently produce $\dot{O}H$ radicals and these promote fuel consumption. The radicals formed can further participate in chain branching pathways leading to heat release. Therefore, the low-temperature chain branching reaction pathways dominate heat release during the first-stage ignition of 124TMB.

The predicted temperature as well as the mole fractions of the major low-temperature species formed during the oxidation of 124TMB are plotted in Fig. 7. Most of the species formed at low temperatures are consumed during the first-stage heat release. This is consistent with the analyses of heat release for each reaction. The reactions during first-stage ignition also lead to the accumulation of H_2O_2, which is relatively stable at low temperatures ($< \sim$850 K). As higher temperatures, H_2O_2 quickly decomposes to two $\dot{O}H$ radicals, leading to significant heat release and helps promote the second-stage ignition.

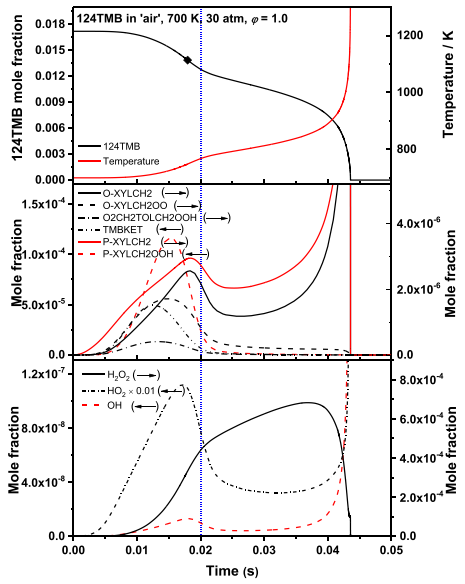

Fig. 7. Temperature and species mole fraction traces for 124TMB at $\varphi = 1.0$ in 'air', 700 K and $p = 30$ atm. Solid symbol: 20% fuel consumption timing.

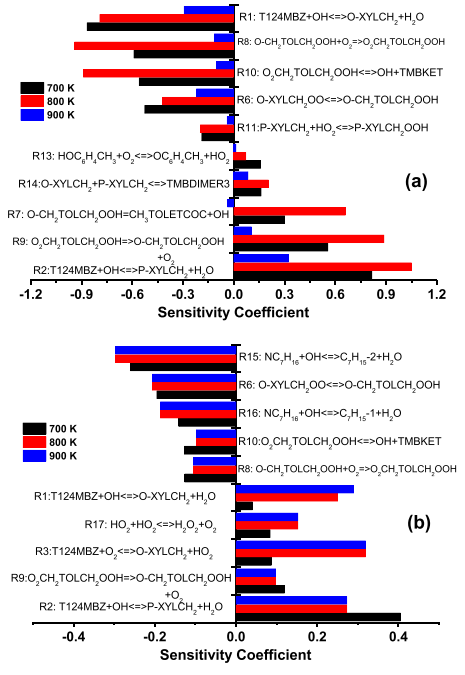

Fig. 8. Sensitivity analyses of IDTs for (a) 124TMB and (b) 75%/25% 124TMB/*n*-heptane blends at $\varphi = 1.0$ in 'air', $p = 30$ atm.

Fig. 8 shows the brute force sensitivity analysis results in which the A-factor of every reaction is perturbed by factor of 2.0 and 0.5. The sensitivity coefficient S_τ is defined as: $S_\tau = \ln(\tau_+/\tau_-)/\ln(k_+/k_-)$ is computed for every reaction. Here k is the original pre-exponential factor of the target reaction; k_+ is the k factor multiplied by 2.0, k_- is the k factor divided by 2.0; τ_+ and τ_- are the corresponding IDTs obtained with k_+ and k_-, respectively. Based on this definition, positive S_τ values indicate reactions that inhibit reactivity and negative values promote reactivity. For pure 124TMB case, H-atom abstraction reactions from 124TMB forming P-XYL$\dot{C}H_2$ (R2) radicals inhibit reactivity, while the abstraction reactions producing O-XYL$\dot{C}H_2$ (R1) promote reactivity. This site-specific effect on ignition propensity is due to reaction R1's ability promote chain branching and chain propagating chemistry. The other reactions with higher sensitivity coefficients which promote reactivity include the formation of $\dot{Q}OOH$ radicals (R6), the second O_2 addition to $\dot{Q}OOH$ radicals (R8), and formation of TMBKET (R10). Reaction R11 also promotes reactivity as it competes with chain terminating reactions such as R14. Strictly speaking, R11 could also be termed a chain termination but the hydroperoxide adduct produced from this reaction subsequently undergoes a unimolecular decomposition reaction to produce $\dot{O}H$ and dimethyl-benzoxyl radical, thus resulting in an overall chain propagating effect. On the other hand, the dimer produced in R14 undergoes H-abstraction reactions and inhibits reactivity. Another reaction class inhibiting reactivity at low temperatures is the decomposition of $\dot{O}_2QOOH$ radicals (R9). Reaction R7, which is the formation of a cyclic-ether from $\dot{Q}OOH$ radicals, inhibits reactivity at 700 K and 800 K as it competes with the second addition to O_2. Interestingly, R7 is found to exhibit a weak reactivity promoting effect at 900 K. This is because at this temperature, the chain branching chemistry is shut-off due to the decreasing stability of $\dot{O}_2QOOH$ radicals with temperature, and the reaction R8 leads to chain propagation.

For the 124TMB/n-heptane blends, abstraction reactions from n-heptane promote reactivity, while abstractions from 124TMB producing both O-XYL$\dot{C}H_2$ and P-XYL$\dot{C}H_2$ radicals inhibit reactivity as seen in Fig. 8b. It is interesting that the sensitivity coefficient of reaction R1 changes from being strongly promoting to inhibiting when the fuel changes from being pure 124TMB to the binary blends. This is because for pure 124TMB, O-XYL$\dot{C}H_2$ provides the chain branching or propagating chemistry from the benzylic $R\dot{O}_2$ chemistry on the *ortho*- sites. While the $R\dot{O}_2$ chemistry from the *ortho*- sites is important, the benzyl $R\dot{O}_2$ radicals are less stable than their alkyl counterparts, as the well depths for $\dot{R} + O_2 \langle = \rangle R\dot{O}_2$ adducts are about 15 kcal/mole lower for benzyl-peroxy radicals compared to alkyl-peroxy radicals. Thus, abstractions from 124TMB by $\dot{O}H$ radicals reduce the reactivity of the binary blends. This change in relative importance of the chemistry with blending shows the importance of the newly acquired binary blend data in the present study.

5. Conclusions

The auto-ignition of 124TMB and its blends with n-heptane has been studied in the low- to intermediate- temperature range at engine relevant conditions using both a HPST and an RCM. The experimental results show that 124TMB presents two-stage ignition behavior at low-temperatures, which is analogous to that of alkane fuels. A detailed kinetic mechanism is proposed and validated against the new experimental IDTs. The new kinetic model can well capture both the first-stage and second-stage ignition behavior. The flux analyses results show that the competitions between chain branching and both chain propagating and chain termination reaction pathways lead to the NTC behavior observed for 124TMB oxidation.

Declaration of Competing Interest

The authors declare that they have no known competing financial interests or personal relationships that could have appeared to influence the work reported in this paper.

Acknowledgements

The work at LLNL was conducted as part of the Partnership to Advance Combustion Engines (PACE) sponsored by the U.S. Department of Energy (DOE) Vehicle Technologies Office, and performed under the auspices of the U.S. DOE, Contract DE-AC52–07NA27344. Jinhu Liang acknowledges the support from the National Natural Science Foundation of China (12172335), International Scientific Cooperation Projects of Key R&D Programs (201803D421101), and Research Project supported by Shanxi Scholarship Council of China (2020-115).The authors at Galway would like to acknowledge Science Foundation Ireland for funding via project number16/SP/3829.

Supplementary materials

Supplementary material associated with this article can be found, in the online version, at doi:10.1016/j.proci.2022.08.106.

References

[1] J.T. Farrell, N.P. Cernansky, F.L. Dryer, C.K. Law, D.G. Friend, C.A. Hergart, R.M. McDavid, A.K. Patel, C.J. Mueller, H. Pitsch, Development of an Experimental Database and Kinetic Models for Surrogate Diesel Fuels, SAE Tech. Pap. 2007 (2007) 776–790.

[2] W.J. Pitz, C.J. Mueller, Recent progress in the development of diesel surrogate fuels, Prog. Energy Combust. Sci. 37 (2011) 330–350.

[3] T. Mitra, C. Chu, A. Naseri, M.J. Thomson, Polycyclic aromatic hydrocarbon formation in a flame of the alkylated aromatic trimethylbenzene compared to those of the alkane dodecane, Combust. Flame. 223 (2021) 495–510.

[4] A. Roubaud, R. Minetti, L.R. Sochet, Oxidation and combustion of low alkylbenzenes at high pressure: comparative reactivity and auto-ignition, Combust. Flame. 121 (2000) 535–541.

[5] P. Diévart, H.H. Kim, S.H. Won, Y. Ju, F.L. Dryer, S. Dooley, W. Wang, M.A. Oehlschlaeger, The combustion properties of 1,3,5-trimethylbenzene and a kinetic model, Fuel 109 (2013) 125–136.

[6] T. Malewicki, S. Gudiyella, K. Brezinsky, Experimental and modeling study on the oxidation of Jet A and the *n*-dodecane/*iso*-octane/*n*-propylbenzene/1,3,5-trimethylbenzene surrogate fuel, Combust. Flame. 160 (2013) 17–30.

[7] E. Ranzi, A. Frassoldati, A. Stagni, M. Pelucchi, A. Cuoci, T. Faravelli, Reduced kinetic schemes of complex reaction systems: fossil and biomass-derived transportation fuels, Inter. J. Chem. Kinet. 46 (2014) 515–542.

[8] J.J. Weng, Y.X. Liu, B.Y. Wang, L.L. Xing, L.D. Zhang, Z.Y. Tian, Experimental and kinetic investigation of 1,2,4-trimethylbenzene oxidation at low temperature, Proc. Combust. Inst. 36 (2017) 909–917.

[9] S. Gaïl, P. Dagaut, Experimental kinetic study of the oxidation of p-xylene in a JSR and comprehensive detailed chemical kinetic modeling, Combust. Flame. 141 (2005) 281–297.

[10] G. Kukkadapu, D. Kang, S.W. Wagnon, K. Zhang, M. Mehl, M. Monge-Palacios, H. Wang, S.S. Goldsborough, C.K. Westbrook, W.J. Pitz, Kinetic modeling study of surrogate components for gasoline, jet and diesel fuels: C7-C11 methylated aromatics, Proc. Combust. Inst. 37 (2019) 521–529.

[11] F. Battin-Leclerc, R. Bounaceur, N. Belmekki, P.A. Glaude, Experimental and modeling study of the oxidation of xylenes, Int. J. Chem. Kinet. 38 (2006) 284–302.

[12] S. Gudiyella, T. Malewicki, A. Comandini, K. Brezinsky, High pressure study of m-xylene oxidation, Combust. Flame. 158 (2011) 687–704.

[13] Y. Li, J. Cai, L. Zhang, J. Yang, Z. Wang, F. Qi, Experimental and modeling investigation on premixed ethylbenzene flames at low pressure, Proc. Combust. Inst. 33 (2011) 617–624.

[14] P. Dagaut, F. Karsenty, G. Dayma, P. Diévart, K. Hadj-Ali, A. Mzé-Ahmed, M. Braun-Unkhoff, J. Herzler, T. Kathrotia, T. Kick, C. Naumann, U. Riedel, L. Thomas, Experimental and detailed kinetic model for the oxidation of a Gas to Liquid (GtL) jet fuel, Combust. Flame. 161 (2014) 835–847.

[15] Z. Wang, Y. Li, F. Zhang, L. Zhang, W. Yuan, Y. Wang, F. Qi, An experimental and kinetic modeling investigation on a rich premixed *n*-propylbenzene flame at low pressure, Proc. Combust. Inst. 34 (2013) 1785–1793.

[16] S. Honnet, K. Seshadri, U. Niemann, N. Peters, A surrogate fuel for kerosene, Proc. Combust. Inst. 32 (I) (2009) 485–492.

[17] E. Riesmeier, S. Honnet, N. Peters, Flamelet modeling of pollutant formation in a gas turbine combustion chamber using detailed chemistry for a kerosene model fuel, J. Eng. Gas Turbines Power. 126 (2004) 899–905.

[18] J.B. Moss, I.M. Aksit, Modelling soot formation in a laminar diffusion flame burning a surrogate kerosene fuel, Proc. Combust. Inst. 31 (II) (2007) 3139–3146.

[19] S. Cheng, C. Saggese, D. Kang, S.S. Goldsborough, S.W. Wagnon, G. Kukkadapu, K. Zhang, M. Mehl, W.J. Pitz, Autoignition and preliminary heat release of gasoline surrogates and their blends with ethanol at engine-relevant conditions: experiments and comprehensive kinetic modeling, Combust. Flame. 228 (2021) 57–77.

[20] S.M. Sarathy, G. Kukkadapu, M. Mehl, T. Javed, A. Ahmed, N. Naser, A. Tekawade, G. Kosiba, M. AlAbbad, E. Singh, S. Park, M. Al Rashidi, S.H. Chung, W.L. Roberts, M.A. Oehlschlaeger, C.J. Sung, A. Farooq, Compositional effects on the ignition of FACE gasolines, Combust. Flame. 169 (2016) 171–193.

[21] G. Bikas, Kinetic Mechanisms for Hydrocarbon Ignition, Ph.D. Thesis, Univerity Achen, Germany, 2001.

[22] D. Darcy, C.J. Tobin, K. Yasunaga, J.M. Simmie, J. Würmel, W.K. Metcalfe, T. Niass, S.S. Ahmed, C.K. Westbrook, H.J. Curran, A high pressure shock tube study of n-propylbenzene oxidation and its comparison with n-butylbenzene, Combust. Flame. 159 (2012) 2219–2232.

[23] D. Darcy, H. Nakamura, C.J. Tobin, M. Mehl, W.K. Metcalfe, W.J. Pitz, C.K. Westbrook, H.J. Curran, A high-pressure rapid compression machine study of n -propylbenzene ignition, Combust. Flame. 161 (2014) 65–74.

[24] C. Morley, GasEq, Version 0.76. http://www.gaseq.co.uk, 2004.

[25] Y. Li, C.W. Zhou, H.J. Curran, An extensive experimental and modeling study of 1-butene oxidation, Combust. Flame 181 (2017) 198–213.

[26] Z. Malliotakis, C. Banyon, K. Zhang, S. Wagnon, J.J. Rodriguez Henriquez, G. Vourliotakis, C. Keramiotis, M. Founti, F. Mauss, W.J. Pitz, H. Curran, Testing the validity of a mechanism describing the oxidation of binary n-heptane/toluene mixtures at engine operating conditions, Combust. Flame. 199 (2019) 241–248.

[27] B. Chen, Z. Wang, J.Y. Wang, H. Wang, C. Togbé, P. Emmanuel, et al., Exploring gasoline oxidation chemistry in jet stirred reactors, Fuel 236 (2019) 1282–1292.

[28] A.N. Morozov, I.A. Medvedkov, V.N. Azyazov, A.M. Mebel, Theoretical Study of the Phenoxy Radical Recombination with the O(3P) Atom, Phenyl plus Molecular Oxygen Revisited, J. Phys. Chem. A. 125 (2021) 3965–3977.

[29] N. Hansen, B. Yang, M. Braun-Unkhoff, A. Ramirez, G. Kukkadapu, Molecular-growth pathways in premixed flames of benzene and toluene

doped with propyne, Combust. Flame. (2022) 112075.
[30] T. Seta, M. Nakajima, A. Miyoshi, High-temperature reactions of OH radicals with benzene and toluene, J. Phys. Chem. A. 110 (2006) 5081–5090.
[31] M.A. Oehlschlaeger, D.F. Davidson, R.K. Hanson, Investigation of the reaction of toluene with molecular oxygen in shock-heated gases, Combust. Flame. 147 (2006) 195–208.
[32] Y. Murakami, T. Oguchi, K. Hashimoto, Y. Nosaka, Theoretical study of the benzyl + O_2 reaction: kinetics, mechanism, and product branching ratios, J. Phys. Chem. A. 111 (2007) 13200–13208.
[33] S. Canneaux, F. Louis, M. Ribaucour, A. El Bakali, J.F. Pauwels, A CASPT2 Theoretical Study of the Kinetics of the 2-, 3-, and 4-Methylbenzylperoxy Radical Isomerization, J. Phys. Chem. A. 113 (2009) 2995–3003.
[34] R. Bounaceur, I. Da Costa, R. Fournet, F. Billaud, F. Battin-Leclerc, Experimental and modeling study of the oxidation of toluene, Int. J. Chem. Kinet. 37 (2005) 25–49.
[35] A. Matsugi, A. Miyoshi, Kinetics of the self-reactions of benzyl and o-xylyl radicals studied by cavity ring-down spectroscopy, Chem. Phys. Lett. 521 (2012) 26–30.
[36] R. Sivaramakrishnan, J. Michael, Rate constants for OH with selected large alkanes: shock-tube measurements and an improved group scheme, J. Phys. Chem. A 113 (2009) 5047–5060.
[37] M. Burke, S.J. Klippenstein, L.B. Harding, A quantitative explanation for the apparent anomalous temperature dependence of $OH+HO_2=H_2O+O_2$ through multi-scale modeling, Proc. Combust. Inst. 34 (2013) 547–555.
[38] G.Da Silva, J.W. Bozzelli, Kinetic modeling of the benzyl + HO_2 reaction, Proc. Combust. Inst. 32 (I) (2009) 287–294.
[39] CHEMKIN-PRO 15101, Reaction Design, San Diego, 2010.
[40] E.J. Silke, H.J. Curran, J.M. Simmie, The influence of fuel structure on combustion as demonstrated by the isomers of heptane: a rapid compression machine study, Proc. Combust. Inst. 30 (2005) 2639–2647.
[41] K.A. Heufer, H. Olivier, Determination of ignition delay times of different hydrocarbons in a new high pressure shock tube, Shock Waves 20 (2010) 307–316.